PAPER

Inverted structural quantum dot light-emitting diodes based on Al-doped ZnO electrode

To cite this article: Zhaobing Tang *et al* 2017 *Nanotechnology* **28** 365201

View the article online for updates and enhancements.

Inverted structural quantum dot light-emitting diodes based on Al-doped ZnO electrode

Zhaobing Tang[1,2]**, Jie Lin**[1,5]**, Lishuang Wang**[1,2]**, Jinsong luo**[1]**, Jialong Zhao**[3,5]**, Haibo Li**[3]**, Yunjun Wang**[4] **and Xingyuan Liu**[1,5]

[1] State Key Laboratory of Luminescence and Applications, Changchun Institute of Optics, Fine Mechanics and Physics, Chinese Academy of Sciences, Changchun 130033, People's Republic of China
[2] University of Chinese Academy of Sciences, Beijing 100049, People's Republic of China
[3] Key Laboratory of Functional Materials Physics and Chemistry of the Ministry of Education, Jilin Normal University, Siping 136000, People's Republic of China
[4] Suzhou Xingshuo Nanotech Co., Ltd, Suzhou 215123, People's Republic of China

E-mail: linj@ciomp.ac.cn, zhaojl@ciomp.ac.cn and liuxy@ciomp.ac.cn

Abstract

As an indium-free transparent conducting film, Al-doped zinc oxide (AZO) was prepared by magnetron sputtering technique, exhibiting good electrical, optical and surface characteristics. UPS/XPS measurements show that AZO and zinc oxide nanoparticles (ZnO NPs) have matched energy level that can facilitate the electron injection from AZO to ZnO NPs. Inverted structural green quantum dot light-emitting diodes based on AZO cathode were fabricated, which exhibits a maximum luminance up to $178\,000$ cd m^{-2}, and a maximum current efficiency of 10.1 cd A^{-1}. Therewith, combined with the simulated space-charge-limited current (SCLC) theory, the measured current density–voltage characteristics of charge-only devices were analyzed. It demonstrated that AZO and ZnO NPs had much better electron injection efficiency than ITO, showing a electron injection efficiency close to 100%. By studying the relationship between the electric field and the current density, the measured curve of AZO-based devices nearly fits the theoretical curve of SCLC and the AZO electrode has a better ohmic contact with ZnO NPs than ITO.

Keywords: AZO, quantum dots, QLEDs, SCLC, space-charge-limited current

(Some figures may appear in colour only in the online journal)

1. Introduction

During the past three decades, colloidal quantum-dot light-emitting diodes (QLEDs) have become promising display technologies for lighting and flat displays owing to their unique characteristics such as tunable narrow linewidth emission, simple preparation process, and high electroluminescence (EL) performance [1–9], which brings about a better color purity and gradually improved EL parameters in green and red QLEDs that close to those of organic light-emitting diodes (OLEDs). Red and green QLEDs with

inverted hybrid sandwich structure were reported to have maximum luminance over $160\,000$ cd m^{-2} and $200\,000$ cd m^{-2}, respectively [10, 11].

EL emission of QLEDs is reliant on the radiative recombination of excitons in emission layer [2, 12]. EL efficiency and luminance depend on the effective injection of charge into quantum dots (QDs), which is related to the bias, the work function of electrodes and the energy barrier between functional materials. At present, indium tin oxide (ITO) is regnant in QLEDs for the great intermingling of low resistance, high transmittance in visible region and mature preparation process. Nevertheless, in OLEDs, the ITO electrode has a negative effect on EL performances owing to the

---

[5] Authors to whom any correspondence should be addressed.

diffusion of indium elements into the device [13], similar effect may also exist in QLEDs with a normal structure that having organic materials next to the ITO layer. Besides, from the view of practicality, transparent electrode of indium with poor flexibility used in QLEDs has a high cost due to the scarcity of indium element. Therefore, it is essential to develop suitable transparent electrodes for low-cost as well as future flexible and high-performance QLEDs. Some emerging electrodes have been adopted in QLEDs, such as graphene [14], silver nanowire [15], fluorine-doped tin oxide [16] and so on. As we know, owing to the good optoelectronic properties including inexpensive, low resistivity and high transmittance in visible light rang [17], nontoxic Al-doped ZnO (AZO) is a kind of transparent conducting oxides that has been used wildly in many display devices as an indium-free transparent electrode [18–20]. In inverted QLEDs, solution-processable ZnO NPs are used as the electron transport layer (ETL) on top of the transparent electrode [21]. But due to the low conduction band of ZnO NPs ($\sim$4.02 eV) [10], ITO as cathode has a higher bias of electron injection. By studying the optical and electrical characteristics, AZO should be a good choice for inverted QLEDs. In other words, the quality of the AZO/ZnO NPs interface is better than that of ITO/ZnO NPs, which facilities effective charge injection and improved EL performance.

Herein, employing an inverted device structure with the AZO electrode, we realized a high-performance green QLEDs with maximum luminance and current efficiency over 178 000 cd m^{-2} and 10 cd A^{-1}, respectively. Also, the AZO based sample has much lower turn-on voltage ($\sim$2.8 V), compared with the reference device. These results have a foundation for the application of indium-free electrode in QLEDs. Furthermore, study charge-only devices with SCLC model, the calculated results show that the AZO has a higher electron injection efficiency than ITO, which is consistent with the results of a close energy level between AZO and ZnO NPs.

2. Experimental section

2.1. Materials

ZnO NPs were prepared in line with the experiment in literature [22]. Molybdenum oxide (MoO$_3$) and cesium carbonate (Cs$_2$CO$_3$) were purchased from regular suppliers. ITO coated glass substrates were purchased from Wuhan Zhuoxin Technology Co., Ltd. Cadmium selenide (CdSe) and zinc sulfide (ZnS) alloyed QDs were provided by Suzhou Xing-shuo Nanotech Co., Ltd. 4,4′-Bis (N-carbazolyl)-1,1′-biphenyl (CBP) was purchased from Xi'an Polymer Light Technology Corp.

2.2. Fabrication of AZO electrode

It is helpful to the preparation of thin film light-emitting device by spin-coating method with thin transparent electrode under the similar optical and electrical properties. The sheet resistance of commercial AZO is about 10 Ω/□, and the thickness of commercial AZO film is about 700–800 nm, which is more than twice the thickness of AZO that we prepared. AZO films were deposited on glass substrates at 200 °C by DC reactive magnetron sputtering. The base pressure in vacuum chamber was 3.0×10^{-4} Pa. An AZO (ZnO: Al$_2$O$_3$ = 98 : 2 wt%) ceramic target was used for the sputtering with a target-substrate distance of 8 cm. The AZO sputtering was carried out at a DC power of 60 W for 90 min in a hybrid Ar/H$_2$ (Ar: H$_2$ = 100 : 5) with an operating vacuum pressure of 1.1 Pa. In order to reduce the influence of impurities, the target was pre-sputtered for 15 min under the same conditions. The as-deposited AZO film has a square resistance of 9.7 Ω/□, which is similar to that of commercialized ITO film. The thickness of AZO and ITO is about 300 nm and 120 nm, respectively. The optical and electrical properties are comparable to the commercial AZO.

2.3. Device fabrication

Fabrication of the QD-LEDs starts with pre-patterned AZO electrode on a glass substrate with active area of 1×1 mm^2, and the contrast device using the ITO electrode. After the substrate is ultrasonically cleaned with acetone, isopropanol and deionized water in sequence for 8 min, a 50 nm thick zinc oxide (ZnO) electron-transport layer is formed by spin-casting ZnO NPs solution onto the substrate and annealing it at 120 °C for 10 min. At last, a about 20 nm thick QD film is spin-coated onto the layer of ZnO NPs at 2500 rpm for 30 s in the same glove box (Mikrouna), followed by annealing at 90 °C for 10 min. The samples are then transferred into a vacuum chamber (with a base pressure of 2×10^{-4} Pa), where a 45 nm thick 4,4′-N,N′-dicarbazolebiphenyl (CBP) hole-transporting layer, a 10 nm thick molybdenum oxide (MoO$_3$) hole-injection layer, and a 100 nm thick aluminum (Al) anode are deposited by sequential thermal evaporation. A 5 nm thick Cs$_2$CO$_3$ layer by spin-coating process at 1500 rpm from a 45 mg ml^{-1} butanol solution and then annealed at 120 °C for 10 min in the glove box.

2.4. Sample characterization

Absorption and transmittance spectra were measured with a Shimadzu UV-3101 spectrophotometer. Photoluminescence (PL) spectrum of QDs in hexane was collected by a Hitachi F-4500 fluorescence spectrophotometer at an excitation wavelength of 340 nm. The surface morphology was evaluated by atomic force microscopy (AFM) images through a Shimadzu SPM-9700 scanning probe microscope in tapping mode. The x-ray diffraction patterns measurements were carried out using a Bruker D8 Focus x-ray diffractometer (Cu Kα, λ = 1.54 Å). The work function of cathodes was investigated by a KP Technology Ambient Kelvin probe system. The sheet resistance of cathodes was measured by a Jandel RM3000 four-point probe. Film thickness was calibrated with an Ambios XP-1 surface profiler. Ultraviolet photoelectron spectroscopy (UPS) spectra were obtained by a Thermo ESCALAB 250 surface analysis system equipped

with a helium discharge lamp at hν = 21.22 eV. X-ray photoelectron spectroscopy (XPS) measurements were performed by a Thermo ESCALAB 250 instrument with Al Kx-rays (hν = 1486.6 eV) to acquire the surface properties. Current density–voltage–luminance (*J–V–L*) characteristics of QLEDs were measured using a Keithley 2611 source meter and a Konica Minolta LS-110 luminance meter. EL spectra were recorded by Avantes Avaspec 2048 spectrometer. All QLED characterizations were carried out at room temperature in ambient atmosphere.

3. Results and discussions

As shown in figure 1(a), the XRD spectrum of AZO film has a primary peak at 34.47° with a full width half maximum (FWHM) of 0.24°, which can be attributed to the (002) peak of the hexagonal-wurtzite-phase ZnO crystal structure (JCPDS card No. 36–1451). Another very weak diffraction peak located at 36.20° with a FWHM of 1.40°, corresponds to ZnO (101) orientation. The dominant (002) peak in the XRD pattern indicates that the as-deposited film has a polycrystalline structure with a preferred orientation in the *c*-axis perpendicular to the plane of the substrate. Average grain size can be estimated by Scherrer's equation:

$$L_c = \frac{K\lambda}{\beta \cos \theta_B},\qquad(1)$$

where, L_c is the mean size of crystalline domains in a film, K (~0.89) is a dimensionless shape factor, λ is the x-ray wavelength (0.154 nm), β is the FWHM, and θ_B is the Bragg diffraction peak. The calculated grain size in the *c*-axis of AZO films is about 39.7 nm.
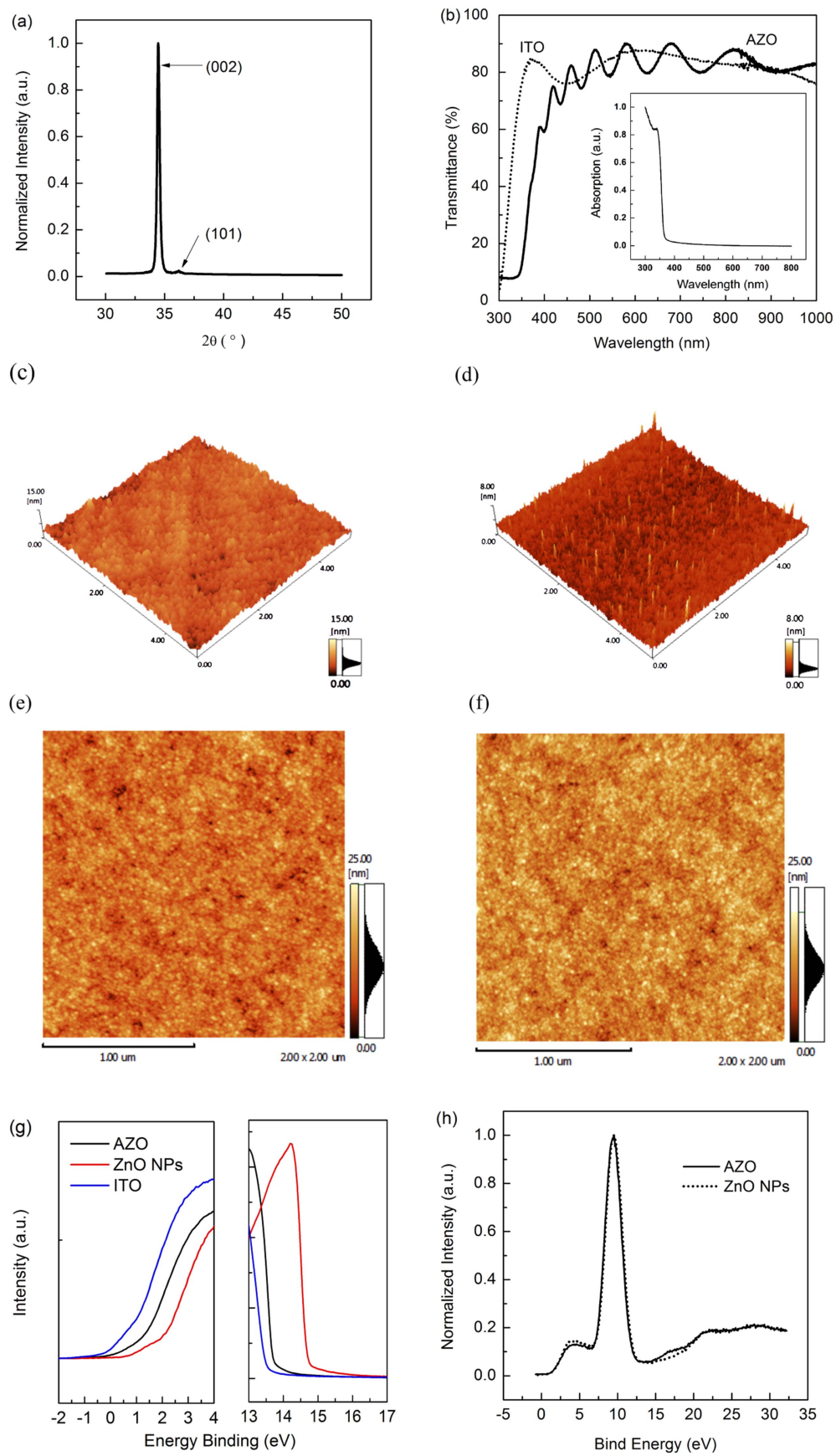
Figure 1(b) compares optical transmittance spectra of AZO and ITO, and shows that AZO film has a maximum transmittance (T_{max}) of 90.1%, 79.9% at the wavelength of 535 nm, and an average transmittance of 81.8% in visible spectral region (400–700 nm). By comparison, ITO has a T_{max} of 87.9%, 83.8% at the wavelength of 535 nm, and an average transmittance of 85.2% in visible spectral region. Hall measurements indicates that AZO film has a resistivity of $2.72 \times 10^{-4}\,\Omega$ cm with an electron concentrations of 1.02×10^{21} cm^{-3} and an electron mobility of 23.22 cm^2 V^{-1} s^{-1}. This electrical characteristic is somewhat lower than that of commercial ITO which has resistivity of $9.37 \times 10^{-5}\,\Omega$ cm with an electron concentrations of 1.91×10^{21} cm^{-3} and an electron mobility of 32.56 cm^2 V^{-1} s^{-1}. While, integrated optoelectronic properties of AZO film are rather close to those of ITO, and meet the requirements of the electrode in QLEDs.

AFM images over a $5 \times 5\,\mu$m^2 area in figures 1(c) and (d) indicate that despite some spikes on the surface of AZO, both AZO and ITO films have smooth surface topography with a surface roughness of 1.31 nm and 0.86 nm, respectively. With spin-coated ZnO NPs over the AZO and ITO layers, surface roughness increases to 2.6 and 2.2 nm, accordingly (figures 1(e) and (f)). UPS measurements were performed to explore the energy levels of AZO, ITO and ZnO

NPs (figure 1(g)). The calculated results indicate that the work function of AZO is 4.65, 0.22 eV less than that of ITO. Based on the further measured absorption spectrum of ZnO NPs (the inset of figure 1(b)), the valence band and conduction band levels of ZnO NPs can be identified as 7.04 eV and 3.65 eV, respectively. The energy level of ZnO NPs is closely related to synthetic conditions. XPS spectra show that AZO and ZnO NPs have roughly the same valence bond levels assigned as Zn 3D for zinc and O 1s for oxygen (figure 1(h)) [19]. As a result, AZO and ZnO NPs have a much lower barrier of electron transition than ITO, which facilitates the electron injection from the Fermi energy level of AZO to the conduction band of ZnO NPs. More exactly, the charge injection efficiency relies not only upon the work function of electrodes but also upon interfacial structure and electron states. AZO has an appropriate work function, belongs to the same material system of ZnO and would have a better lattice matching with ZnO NPs than ITO. Therefore, AZO is an advisable cathode for inverted structural QLEDs. Considering that the ZnO NP film has a good electron mobility ($\mu_e \sim 1.3 \times 10^{-3}$ cm^2 V^{-1} s^{-1}), it is suitable to use 4,4′-Bis(N-carbazolyl)-1,1′-biphenyl (CBP) as HTL because the hole mobility of CBP ($\mu_h \sim 1.0 \times 10^{-3}$ cm^2 V^{-1} s^{-1}) is comparable to the electron mobility of ZnO NPs. This helps to the balance injection of electrons and holes into QDs, so as to improve the EL efficiency [10].
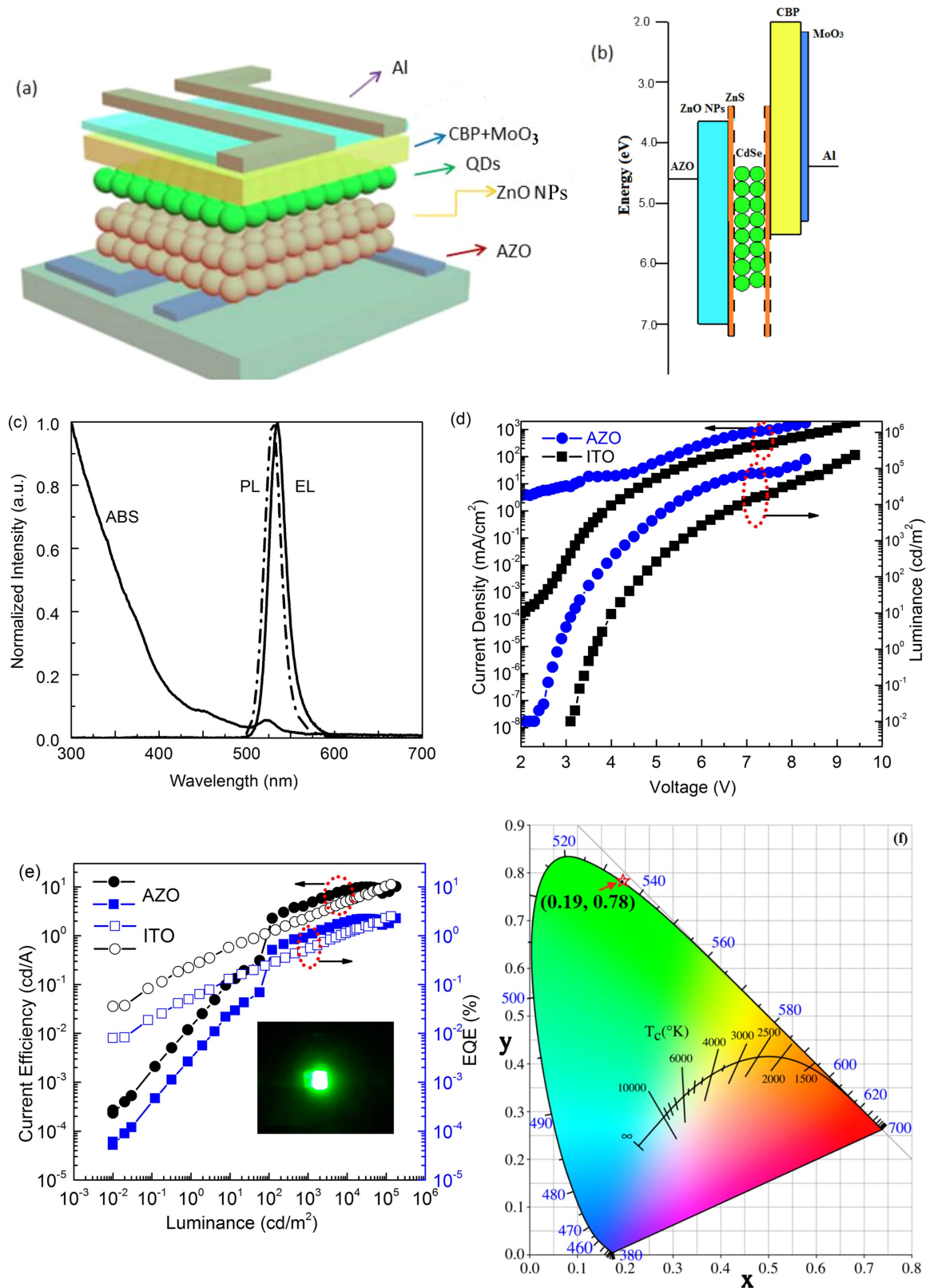
Inverted structural QLEDs were fabricated by employing AZO as a contact cathode. Simultaneously, the reference device was prepared with ITO as cathode. A schematic structure and energy band diagram of AZO-based QLEDs with a multilayered structure are shown in figures 2(a) and (b). The used CdSe/ZnS core/shell QDs possess a PL quantum yield of 70%. Figure 2(c) shows that the QDs have a PL peak at 529 nm with a FWHM of 22.5 nm, and two small absorption peaks at 452 nm and 523 nm, respectively, in visible region, and strong absorption in UV spectral region. EL spectrum shows an emission peak at 535 nm with a FWHM of 22.6 nm, which displays a good saturated color emission according to the 1931 Commission Internationale de Eclairage chromaticity diagram (figure 2(f)). Red-shift of EL spectrum with respect to PL spectrum can be attributed to inter-dot interaction or the electric-field-induced Stark effect. In close packing QDs solid, electronic energy transfer would emerge for the inhomogeneous sample because the particle size of QDs cannot be identical absolutely and dipole–dipole inter-dot interactions could induce the long-range resonance transfer [23].

Electrodes can affect the EL performance of QLEDs greatly. The curves of *J–V–L* and CE–V of inverted QLEDs in figures 2(d) and (e) shows that the AZO-based device has a higher current density of 792 mA cm^{-2} than the ITO-based reference device (218 mA cm^{-2}) at the same voltage of 7 V, which is consistent with the fact of lower barrier of electron transition at the interface of AZO/ZnO NPs. It can be speculated that the electron injection from AZO cathode to ZnO NPs is rather effective, leading to a high current density under the same voltage in comparison to the reference device. Similarly, the AZO-based device shows a turn-on voltage
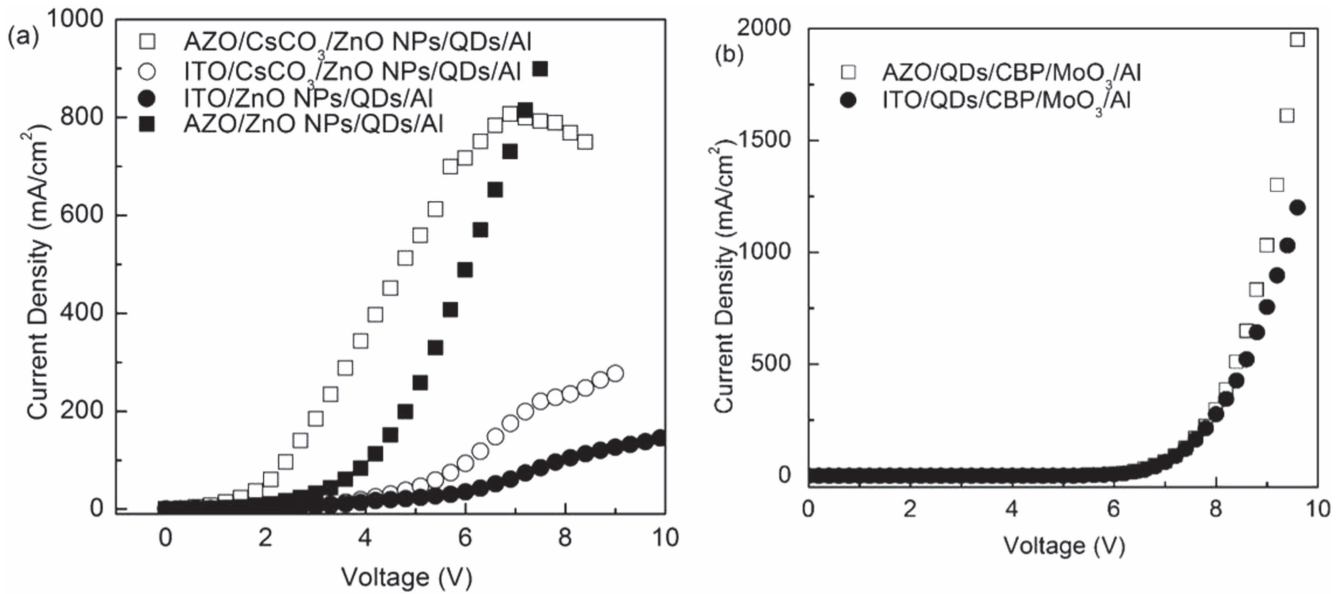
Figure 1. (a) XRD pattern of AZO film. (b) Transmittance spectra of AZO and ITO films. (c) AFM image of AZO film. (d) AFM image of ITO film. (e) AFM image of ZnO NPs on AZO. (f) AFM image of ZnO NPs on ITO. (g) UPS spectra of AZO, ITO and ZnO NPs. (h) XPS spectra of AZO and ZnO NPs.

Figure 2. (a) Schematic architecture of QLEDs. (b) Flat-band energy level diagram. (c) The normalized absorption and PL spectra of QDs, and EL spectrum of QLED. (d) Current density–voltage–luminance (*J–V–L*) characteristics of QLEDs based on AZO and ITO cathodes. (e) Current efficiency–luminance–EQE (CE–*L*–EQE) characteristics; the inset is the photograph of AZO based QLEDs at 6 V. (f) CIE coordinate of QLEDs.

Figure 3. (a) Electron-only devices. (b) Hole-only devices. The thicknesses of each layers are identical to those in the optimized QLEDs.

(V_{on}) of 2.8 V, about 1.1 V lower than that of the reference device. While the maximum luminance of 178 000 cd m^{-2} for the AZO-based device is inferior to that of 233 000 cd m^{-2} for the reference device, and the former device reach its maximum luminance and maximum efficiency at 8.4 V and 6.3 V, respectively, which is reduced by 1 V and 3 V, respectively, compared to the reference device.

However, the maximum CE of 10.1 cd A^{-1} for the AZO-based device is lower than that of 12.2 cd A^{-1} for the reference device, the CE at 6 V for the former device is 9.9 cd A^{-1}, higher than the later (3.4 cd A^{-1}) at the same voltage. Specifically, the AZO-based device shows a higher current density, luminance, and CE than the reference device under the same voltage, which indicates a very efficient electron injection from AZO cathode to ETL. AZO-based device has the external quantum efficiency (EQE) of 2.3% that is almost the same as the EQE of reference device (2.5%). It is well known that the *J–V* curve of QLEDs showed ohmic conduction, trap-limited conduction and space-charge limited conduction at relatively low voltage, medium voltage and high voltage in sequence [24]. The voltage for AZO-based QLED corresponding to trap-limited conduction is lower than that for the reference device, which shows that there is a better interface between AZO and ZnO NPs. A decrease of CE after around 6 V in AZO-based device originates from excessive electron injection and the EL efficiency characteristics under space-charge limited conduction mechanism.
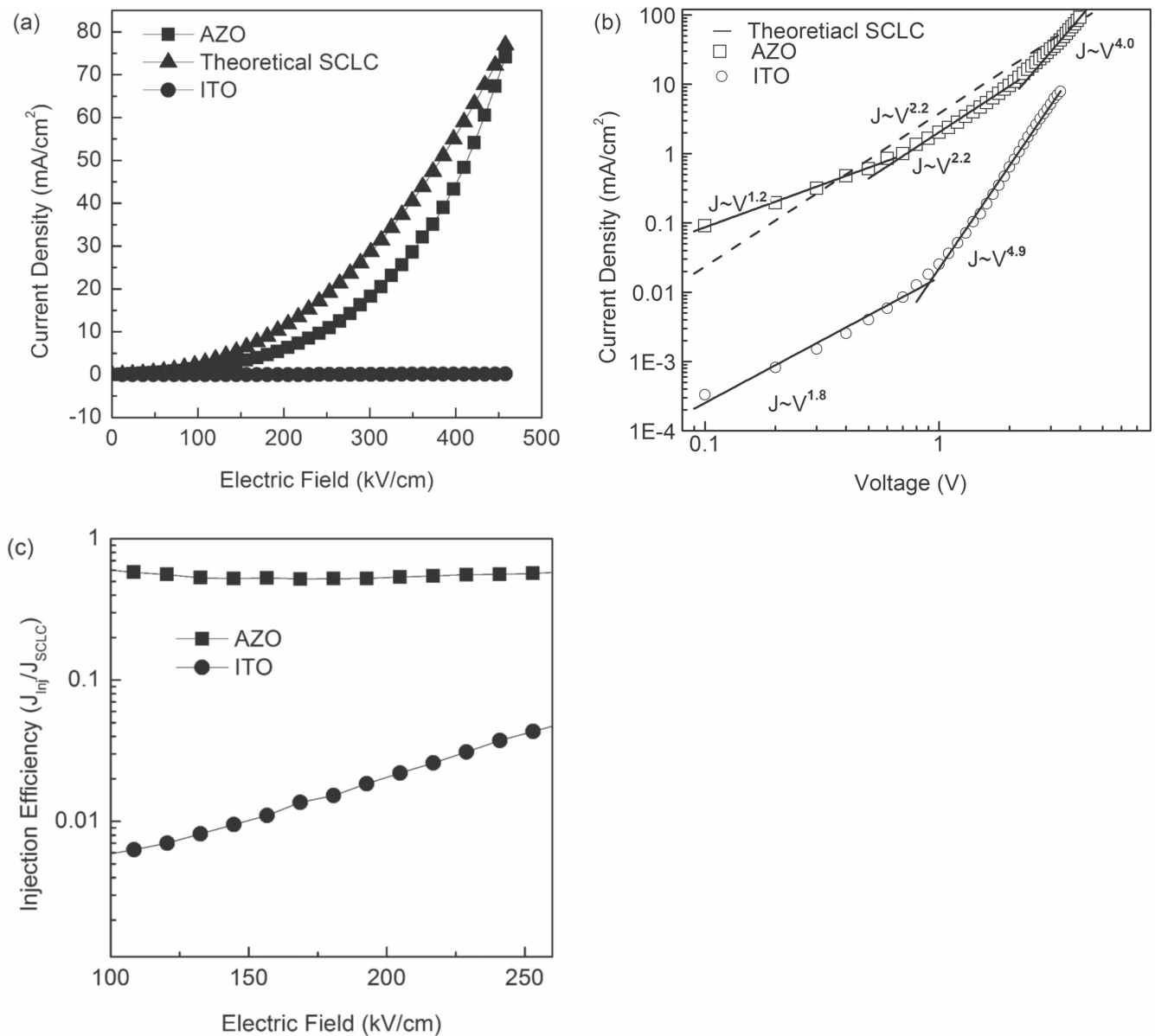
We suggest that the Fermi energy level of AZO is close to the conduction level of ZnO NPs, which brings about good interface for the effective injection of electrons. To investigate charge injection characteristics of transparent cathodes, electron-only and hole-only devices were fabricated. Because Cs_2CO_3 material can form a low work function interface to facilitate electron injection [25, 26]. Cs_2CO_3 thin film was added between cathodes and ZnO NPs. *J–V* properties of charge-only devices are showed in figure 3. For electron-only

devices, the current density of the AZO-based device is significantly higher than ITO-based one, which is an order of magnitude higher at the voltage of 2 V, and shows more efficient electron injection between AZO/ZnO NPs. After adding the Cs_2CO_3 layer, the current density of both AZO/ITO-based devices increase quickly as the voltage rises, resulting from the reduced work function of cathodes. But current density of AZO-based device begins to decrease with the further increase of voltage owing to the fast accumulation of space charge. For similar reasons, the rising of current density of ITO-based device shows a reduced slope at the high voltage stage with or without Cs_2CO_3 layer. The current density of the two hole-only devices has the similar trend with the variable voltage, but AZO-based device has slightly higher current density. Comparing to electron-only device, the current density of corresponding hole-only device increases rapidly at a high voltage stage. The experimental results show that the current density of AZO-based electron/hole-only devices is higher than ITO-based ones at the same voltage.

To further study electron-only device, assuming an ohmic injection contact between the layers, the electron injection behavior was analyzed by the theory of space-charge-limited current density (J_{SCLC}) with Frenkel effect as follows [27]:

$$J_{SCLC} = \frac{9}{8}\mu_0\varepsilon_0\varepsilon_r \exp\left(0.89\beta\sqrt{V/d}\right)\frac{V^2}{d^3}, \qquad (2)$$

where, μ_0, ε_0, ε_r, and are the zero-field mobility, the vacuum permittivity and the relative permittivity, respectively. β is a constant of temperature-related, which is equal to 1.3×10^{-3} (cm/V)$^{-2}$ here. V is the applied voltage and d is the distance between electrodes. Frenkel effect refers to the effective depth of trap that decreases at the intense electric field. The theoretical J_{SCLC} is obtained from the equation (2). Figure 4(a) shows the curve of current density–electric field

Figure 4. (a) The curves of current density–electric field for electron-only device. (b) The *J–V* curves of electron-only devices on log–log scale. (c) The dependence of electron injection efficiency on electric field based on SCLC model.

(*J–E*) for the AZO/ITO-based devices and indicates that the current density of the AZO-based device is enhanced distinctly in comparison to that of ITO-based device with the similar architecture. The *J–E* curve of AZO-based device is coincident well with the theoretical J_{SCLC} curve. Simultaneously, the *J–V* curves in figure 4(b) meets the power variation law under trap charge limited [28], which obeys ohmic conduction at lower voltage, with increasing voltage, and higher power law at higher voltage [29]. From the fitting curves, the power value of applied voltage for the ITO-based device is far above AZO-based device, which suggests a deep trap states at the ITO/ZnO NPs interface. So AZO/ZnO NPs has a better interface contact as well as a more matching energy level than ITO/ZnO NPs. As shown in figure 4(c), electron injection efficiency was calculated by $\eta_{inj} = J_{inj}/J_{SCLC}$, where J_{inj} and J_{SCLC} are the measured current density and the calculated theoretical value of

J_{SCLC}. The high electron injection efficiency of AZO-based device indicates that AZO cathode has formed nearly ohmic contact with ZnO NP layer [30].

4. Conclusion

In this work, electrical and optical properties of magnetron sputtering-prepared AZO has been compared to that of commercial ITO. QLEDs with inverted structure were fabricated based on AZO/ITO cathodes. AZO-based devices show a better luminance and current efficiency than ITO-based devices under the same voltage. On the basis of SCLC model, UPS/XPS test and the measured current density–voltage characteristics of electron-only and hole-only devices, AZO shows a matching energy level with ETL of ZnO NPs and

nearly ohmic contact at the AZO/ZnO NPs interface, and thus exhibits much better charge-injection ability, especially electron injection ability than ITO. Consequently, AZO would have a widely practical application in inverted QLEDs because of its series of advantages including indium-free electrode, low cost, good electrical and optical characteristics, better compatibility with ZnO-based electron transport materials.

Acknowledgments

References

[1] Bozyigit D and Wood V 2013 Challenges and solutions for high-efficiency quantum dot-based LEDs *MRS Bull.* **38** 731–6

[2] Shirasaki Y, Supran G J, Bawendi M G and Bulović V 2012 Emergence of colloidal quantum-dot light-emitting technologies *Nat. Photon.* **7** 13–23

[3] Demir H V, Nizamoglu S, Erdem T, Mutlugun E, Gaponik N and Eychmüller A 2011 Quantum dot integrated LEDs using photonic and excitonic color conversion *Nano Today* **6** 632–47

[4] Supran G J, Shirasaki Y, Song K W, Caruge J M, Kazlas P T, Coe-Sullivan S, Andrew T L, Bawendi M G and Bulovic V 2013 QLEDs for displays and solid-state lighting *MRS Bull.* **38** 703–11

[5] Coe-Sullivan S 2009 Quantum dot developments *Nat. Photon.* **3** 315–6

[6] Coe-Sullivan S, Liu W H, Allen P and Steckel J S 2013 Quantum dots for LED downconversion in display applications *ECS J. Solid State Sci. Technol.* **2** R3026–30

[7] Bera D, Qian L, Tseng T K and Holloway P H 2010 Quantum dots and their multimodal applications: a review *Materials* **3** 2260–345

[8] Dai X, Zhang Z, Jin Y, Niu Y, Cao H, Liang X, Chen L, Wang J and Peng X 2014 Solution-processed, high-performance light-emitting diodes based on quantum dots *Nature* **515** 96–9

[9] Haverinen H M, Myllyla R A and Jabbour G E 2010 Inkjet printed RGB quantum dot-hybrid LED *J. Display Technol.* **6** 87–9

[10] Kwak J *et al* 2012 Bright and efficient full-color colloidal quantum dot light-emitting diodes using an inverted device structure *Nano Lett.* **12** 2362–6

[11] Dong Y *et al* 2015 Ultra-bright, highly efficient, low roll-off inverted quantum-dot light emitting devices (QLEDs) *SID Symp. Digest of Technical Papers* vol 46, pp 270–3

[12] Cho S H, Sung J, Hwang I, Kim R H, Choi Y S, Jo S S, Lee T W and Park C 2012 High performance AC electroluminescence from colloidal quantum dot hybrids *Adv. Mater.* **24** 4540–6

[13] Dugrenil B *et al* 2014 *Organic Photonics VI* ed B P Rand *et al* (Bellingham, WA: SPIE) (https://doi.org/10.1117/12.2052504)

[14] Altintas Y, Genc S, Talpur M Y and Mutlugun E 2016 CdSe/ZnS quantum dot films for high performance flexible lighting and display applications *Nanotechnology* **27** 295604

[15] Lee K-H, Seo J-T, Han J and Lim T 2014 Fully transparent quantum dot light-emitting diode integrated with graphene anode and cathode *ACS Nano* **8** 12476–82

[16] Jing P, Ji W, Zeng Q, Li D, Qu S, Wang J and Zhang D 2015 Vacuum-free transparent quantum dot light-emitting diodes with silver nanowire cathode *Sci. Rep.* **5** 12499

[17] Andersson A, Johansson N, Broms P, Yu N, Lupo D and Salaneck W R 1998 Fluorine tin oxide as an alternative to indium tin oxide in polymer LEDs *Adv. Mater.* **10** 859

[18] Park J W, Oh M S, Park S J, Yoo Y and Kim D Y 2014 Aluminum-doped zinc oxide anode for organic light emitting diodes grown by pulsed laser deposition using plasma-enhanced oxygen radicals *J. Nanoelectron. Optoelectron.* **9** 162–6

[19] You Q H, Cai H, Gao K, Hu Z G, Guo S, Liang P P, Sun J, Xu N and Wu J 2015 Highly transparent and conductive Al-doped ZnO films synthesized by pulsed laser co-ablation of Zn and Al targets assisted by oxygen plasma *J. Alloys Compd.* **626** 415–20

[20] Chauhan R N, Anand R S and Kumar J 2014 RF-sputtered Al-doped ZnO thin films: optoelectrical properties and application in photovoltaic devices *Phys. Status Solidi* a **211** 2514–22

[21] Gentle A R, Yambem S D, Smith G B, Burn P L and Meredith P 2015 Optimized multilayer indium-free electrodes for organic photovoltaics *Phys. Status Solidi* a **212** 348–55

[22] Qian L, Zheng Y, Xue J G and Holloway P H 2011 Stable and efficient quantum-dot light-emitting diodes based on solution-processed multilayer structures *Nat. Photon.* **5** 543–8

[23] Ji W, Jing P, Zhang L, Li D, Zeng Q, Qu S and Zhao J 2014 The work mechanism and sub-bandgap-voltage electroluminescence in inverted quantum dot light-emitting diodes *Sci. Rep.* **4** 6974

[24] Kagan C R, Murray C B and Bawendi M G 1996 Long-range resonance transfer of electronic excitations in close-packed CdSe quantum-dot solids *Phys. Rev.* B **54** 8633–43

[25] Cho K S *et al* 2009 High-performance crosslinked colloidal quantum-dot light-emitting diodes *Nat. Photon.* **3** 341–5

[26] Huang J S, Xu Z and Yang Y 2007 Low-work-function surface formed by solution-processed and thermally deposited nanoscale layers of cesium carbonate *Adv. Funct. Mater.* **17** 1966–73

[27] Small C E, Tsang S-W, Kido J, So S K and So F 2012 Origin of enhanced hole injection in inverted organic devices with electron accepting interlayer *Adv. Funct. Mater.* **22** 3261–6

[28] Murgatroyd P N 1970 Theory of space-charge-limited current enhanced by Frenkel effect *J. Phys. D: Appl. Phys.* **3** 151

[29] Burrows P E, Shen Z, Bulovic V, McCarty D M, Forrest S R, Cronin J A and Thompson M E 1996 Relationship between electroluminescence and current transport in organic heterojunction light-emitting devices *J. Appl. Phys.* **79** 7991–8006

[30] Shi S W and Silva S R P 2012 High luminance organic light-emitting diodes with efficient multi-walled carbon nanotube hole injectors *Carbon* **50** 4163–70